Original Article

Designing and Comparing Performances of Image Processing Pipeline for Enhancement of I-131-metaiodobenzylguanidine Images

Anil Kumar Pandey, Shweta Dhiman, Sreedharan Thankarajan ArunRaj, Chetan Patel, Chandrashekhar Bal, Rakesh Kumar

Department of Nuclear Medicine, All India Institute of Medical Sciences, New Delhi, India

Abstract:

Objective: An image processing pipeline can have more than one image processing technique in sequence, and the output of the first technique becomes input for the next technique and so on. In this study, we have designed and compared the performances of image processing pipelines for enhancement of I-131-metaiodobenzylguanidine (mIBG) images. **Materials and Methods:** Five different image processing pipelines (A [Gaussian filter, normalization], B [histogram specification (image 1), Gaussian filter, normalization], C [histogram specification (image 2), Gaussian filter, normalization], D [{histogram specification (image 3), Gaussian filter, and normalization], and E [histogram specification (image 4), Gaussian filter, normalization]) were designed and their performances were evaluated on I-131-mIBG images (n = 122). The image quality was assessed objectively using Perception-based Image Quality Evaluator (PIQE) score and subjectively (on scale 1–4) by two nuclear medicine physician. Sign test was applied to find the statistically significant difference between the image quality obtained using image processing pipelines. We applied test of proportion to compute difference in proportion of image quality score assigned to images obtained using image processing pipelines. **Results:** Based on PIQE score, the quality of images obtained using all the five image processing pipelines were significantly better than that of input images ($P < 0.001$). The highest image quality score (=4) was assigned maximum number of times (n = 90) to the images obtained using image processing pipeline D and was significantly different from that of the second best image processing pipeline E (P = 0.015). **Conclusions:** The image processing pipeline D was found to be better for enhancement of I-131-mIBG images.

Keywords: *I-131-metaiodobenzylguanidine images, image enhancement, image processing pipeline*

Introduction

Radiolabeled catecholamine analog metaiodobenzylguanidine (MIBG) is widely used to image various tumors of sympathetic nervous system such as pheochromocytomas, neuroblastomas, paragangliomas, and ganglioneuroblastomas. It is also used in other neural crest tumors such as medullary cancer of thyroid and carcinoids. MIBG uptake into these tumor cells occurs by both active and passive mechanisms. Active transport of MIBG into the cell occurs through uptake 1 system and subsequently accumulated in the neurosecretory granules within through vesicular monoamine transporters 1 and 2. The mIBG is labeled with either I-123 or I-131. I-123-mIBG is the radiopharmaceutical of choice because of its short half-life (13.22 h) and energy 159 keV suitable for gamma camera.[1,2] However, the availability of this radiopharmaceutical is limited, and hence, at our center, I-131-mIBG is used.

High-energy beta-particle emission delivers high radiation dose to the patients, and hence, very less amount approximately 2 mCi (74 MBq) of I-131-mIBG dose is administered to the patients to perform a diagnostic scan. The 364 KeV photons are not optimal for imaging on gamma cameras. The count detection sensitivity for I-131 is poor: approximately, half of the photons penetrate the typical three-eighths-inch crystal and thus are not detected. For example, Figure 1a and b show the distribution of total counts acquired in anterior (n = 61) and posterior (n = 61) I-131-mIBG whole-body images included in this study. It can be observed that majority of images have total counts <150 k. Figure 1c and d show anterior image (visually appears dark)

How to cite this article: Pandey AK, Dhiman S, ArunRaj ST, Patel C, Bal C, Kumar R. Designing and comparing performances of image processing pipeline for enhancement of I-131-metaiodobenzylguanidine images. Indian J Nucl Med 2021;36:125-33.

Address for correspondence:
Dr. Anil Kumar Pandey, Department of Nuclear Medicine, All India Institute of Medical Sciences, New Delhi - 110 029, India.
E-mail: akpandeyaiims@gmail.com

Received: 12-12-2020
Revised: 11-02-2021
Accepted: 24-02-2021
Published: 21-06-2021

Access this article online

Website: www.ijnm.in

DOI: 10.4103/ijnm.ijnm_231_20

Quick Response Code:

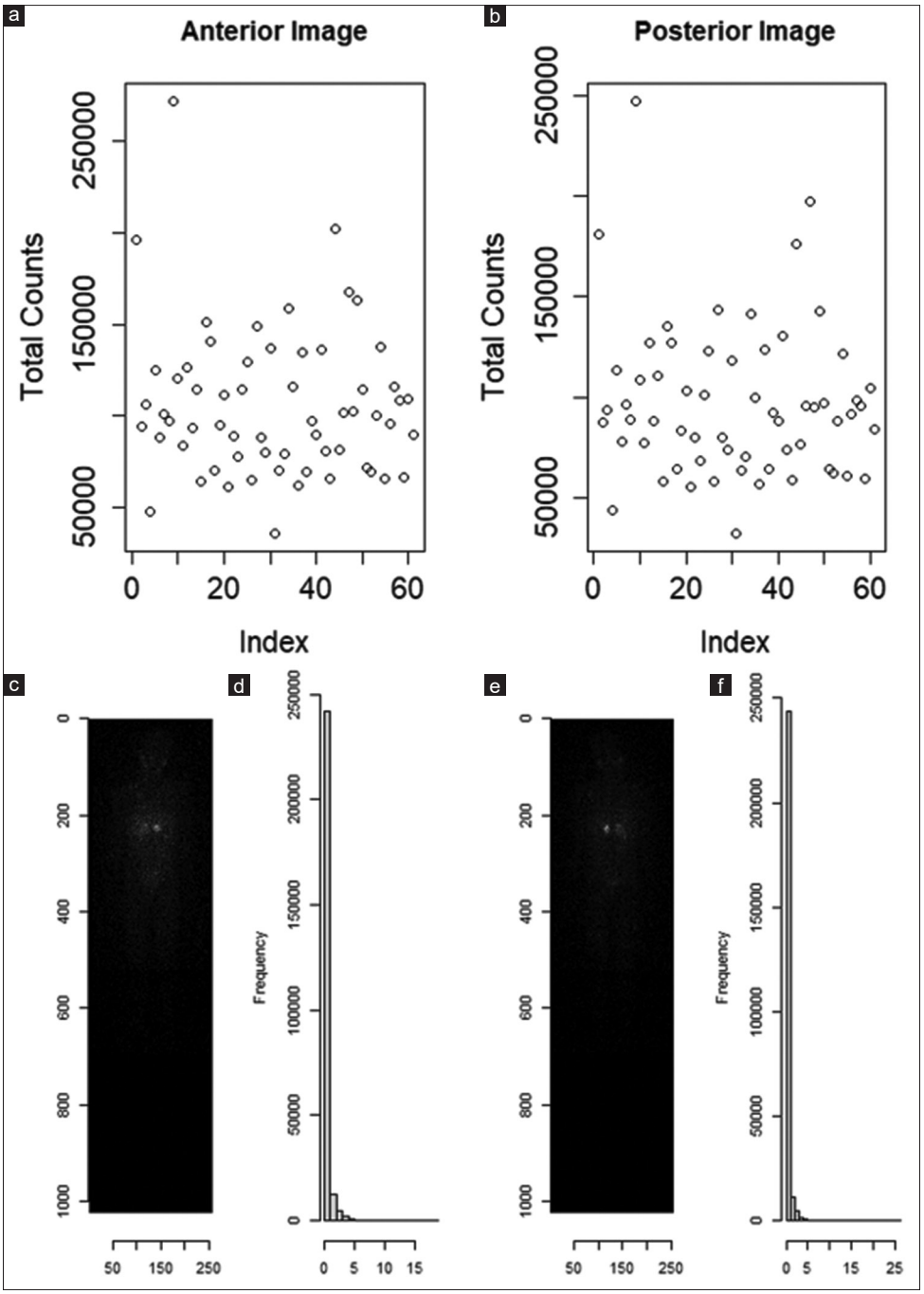

Figure 1: (a) Plot of total counts of anterior images (*n* = 61), (b) plot of total counts of posterior images (*n* = 61), (c) sample of anterior image, (d) histogram of image c, maximum counts = 19, (e) sample of posterior image, (f) histogram of image e, maximum counts = 26. In a and b, x-axis: image index number and y-axis: the corresponding total counts observed in the image. In d and f, x-axis: pixel counts and y-axis: the frequency of pixel counts. In c and e, x-axis: pixel index in x-direction and y-axis: pixel index in y-direction

and its histogram, respectively; Figure 1e and f show posterior image (visually appears dark) and its histogram, respectively.

The image quality is further degraded as a result of detection of scattered and penetrated photons (as a result of interaction of high-energy photons [364 keV] with high-energy parallel hole collimator) in the photopeak window of I-131 (364% ± 20% keV).

I-131-mIBG images acquired with short time period suffer from noise. The noise appears as mask of pixels of random intensities imposed on initial image. Visually, it looks like set of granules which have different sizes, randomly are located at the image, and distorts the actual content of the image. Especially, noise is noticeable on homogeneous or dark image areas.[3-5] The presence of noise worsens visual perception and image analysis. The image with good contrast and detail is required for making diagnosis. Long time

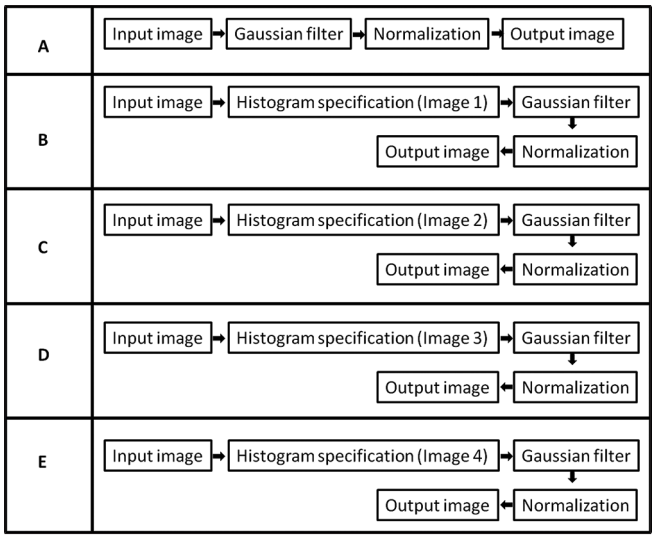

Figure 2: Image processing pipelines used in this study. Histogram specification (image 1) means that histogram specification technique was applied to the input image with input parameter "histogram of image 1." Similarly, histogram specification (image 2) means that histogram specification technique was applied to input image with input parameter "histogram of image 2" and so on. The images 1, 2, 3, and 4 and their histogram is given in Figure 3

period of acquisition can be used to increases the number of detected photons (i.e., to improve the image quality) but is often impractical, due to patient's motion.

Denoising and contrast enhancement operations are two of the most common and important techniques for medical image quality improvement. Because of their importance, there has been an enormous amount of research dedicated to the subject of noise removal and image enhancement.[6-9] It has been reported that when different image enhancement techniques are combined and applied to complex image enhancement task, they produce much better result.[3,10]

The objective of the study was to design and optimize image processing pipelines for enhancing the quality of I-131-mIBG images.

Materials and Methods

The image processing pipeline encompasses a sequence of operations ranging from low-level denoising and sharpening to high-level adjustment and corrections.[11] Five image processing pipelines [Figure 2] were designed and their performance was evaluated on an image database which consists of 61 whole-body I-131 scans.

The four images (these images are not subset of the image database used for evaluating the performance of image processing pipeline) and its histogram which were used in histogram specification are shown in Figure 3. The selection of good quality I-131 images was based on the expectation that the resultant image after histogram specification will have quality similar to these images; however, it should not be far from the characteristic of input image.[12]

The 61 I-131-mIBG whole-body scans were the scans of the patients who were referred to our center for routine I-131-mIBG diagnostic scan. The acquisition protocol used to acquire these scans was the following: *"The patients were given a blocking dose of saturated solution of potassium iodide before administering the radiopharmaceutical. ^{131}I-MIBG was administered intravenously. The dose administered was between 1.2 mCi and 2.2 mCi (40 MBq–80 MBq). The image was acquired 48–72 h after the radiopharmaceutical administration. The images were acquired on GE Discovery 670 NM/CT (General Electrical Healthcare, Illinois, USA). The imaging was performed using high-energy general purpose collimator. Whole-body images were acquired at a scan speed of 10 cm/min in continuous mode or 240 s/step in step and shoot mode with 1024 × 256 matrix size."*

These 61 studies (122 images: 61 anterior and 61 posterior) were exported in DICOM format from the nuclear medicine image processing computer. Nuclear medicine processing computer was used only for exporting the studies into DICOM format, and rest of the experiments were conducted on personal computer. The personal computer had MATLAB R2019b and R statistical software. The image processing pipelines were implemented in R[13] using *Imager*[14] and *EBImage*[15] package.

Venkatanath *et al*.[16] proposed and evaluated a method to evaluate the image quality that does not require reference image. The method computes visual perception-based features from them image and converts them into a score in the range 0–100. They have validated the performance of the method with human observers. Based on the study published by Venkatanath *et al*.,[16] MATLAB has a function named "*piqe*" (Perception-based Image Quality Evaluator [PIQE] no-reference image quality score). A low score value indicates high perceptual quality, and high score value indicates low perceptual quality.[17]

The quality of output images was assessed objectively with *PIQE* score and subjectively two nuclear medicine physicians. Two nuclear medicine physicians reviewed these images under ambient lighting condition. They assigned the score from 1 to 4, 1 being the very poor quality and 4 being the best. The conflict if any was resolved after discussing, and a unanimous image quality score was assigned to each image. The image quality scores for each image were recorded and statistically analyzed.

For statistical analysis, R[13] installed on personal computer was used. For sign test, the package BSDA (basic statistics and data analysis) was used.[18] For proportion test, the base package R was used.[13]

We set up the hypothesis like this – H0: $P = 0.5$, null hypothesis: there is no difference between the two processing methods and H1: $P \neq 0.5$, alternative

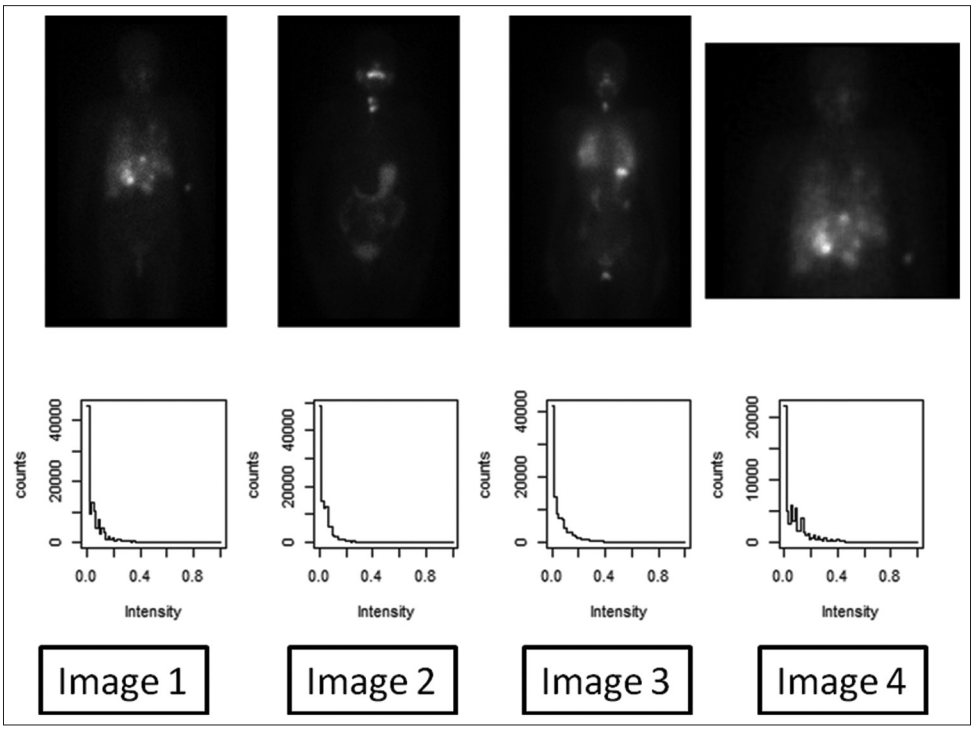

Figure 3: The image (top row) and its corresponding histogram (bottom row) used during histogram specification method. Image 4 was obtained as a result of cropping the image 1 by retaining only the upper half of the body (from head to abdomen). Image 4 was included in this study purposely because even though image 4 was part of image 1, the histogram of image 4 differs (on visual inspection) from the histogram of image 1, and this in turns affect the image quality

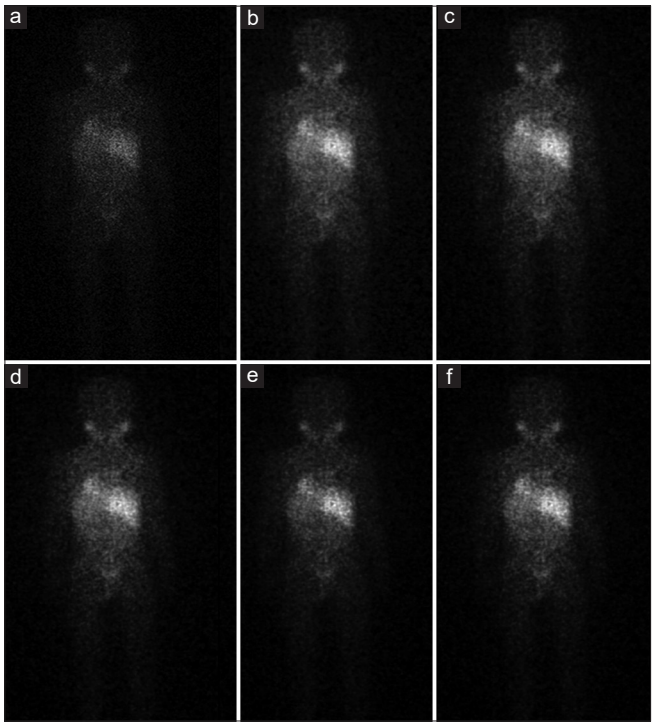

Figure 4: (a) Input image (NMP score = 1, PIQE score = 80.53) (b) output image from image processing pipeline (A) (NMP score = 2, PIQE score = 23.40), (c) output image from processing pipeline (B) (NMP score = 3, PIQE score = 25.72), (d) output image from processing pipeline (C) (NMP score = 3, PIQE score = 26.05), (e) output image from processing pipeline (D) (NMP score = 4, PIQE score = 21.54) and (f) output image from processing pipeline (E) (NMP score = 4, PIQE score = 27.23)

hypothesis: there is a difference between the two types of processing method. Two-tailed dependent samples sign test was applied to find the statistically significant difference between the median image quality score of the images processed using different methods.

Test of proportion (prop. test from R base package) was applied to find the significant difference in the proportion of particular image quality score assigned to the images obtained using two different image processing pipelines.

Results

The performance of image processing pipeline (D) was found to be superior in comparison with all other image processing pipelines [Figure 4]. The output image obtained using image processing pipeline (D) and image processing pipeline (E) received the highest image quality score 4 based on visual assessment [Figure 4]; however, PIQE score was smaller for image processing pipeline (D) indicating better performance compared to image processing pipeline (E). In this case, there was concordance between the result of objective and subjective assessment.

Figure 5 shows an example of input and output images where there was discordance between result of objective and subjective assessment. In this case, nuclear medicine physician assigned highest score assigned to the image obtained using image processing pipeline (a) while based on *PIQE* score, the perceptual quality of image obtained

using image processing pipeline (d) was excellent and the perceptual quality of image obtained using image processing pipeline (a) which is superior was good. It is to be remember that MATLAB function documentation categorizes the image quality into five category-based *PIQE* score of the image whose "quality scale (score range)" are: *Excellent* (0, 20)*, good* (21, 35), *fair* (36, 50), *poor* (51, 80), and *bad* (81, 100).

There was only one input image that received highest image quality score as per visual assessment made by nuclear medicine physicians [Figure 6]. However, based on PIQE score, the output image obtained using image processing pipeline (D) was found to have the best image quality and was labeled as excellent [Figure 6].

Qualitative image quality assessment

The summary statistics of the image quality score assigned by nuclear medicine physicians [Table 1] shows that the images obtained using image processing pipeline (D) and image processing pipeline (E) were competitive and better than the images obtained using other image processing pipeline.

There was statistically significant difference between the median image quality score assigned to images obtained using image processing pipeline (D) and image processing pipeline (E) at $P = 0.000156$. There was statistically significant difference between the median image quality score of the input image and the median image quality score of images obtained using image processing pipeline (D) ($P < 0.00001$). Similarly, there was statistically significant difference between the median image quality score of the input image and the median image quality score of image obtained using image processing pipeline (E) ($P < 0.00001$).

Table 2 shows the number of times a particular image quality score assigned to input and output images obtained using different image processing pipelines (A, B, C, D, and E). The inspection of Table 2 shows that the quality of 96 image improved (their image quality score changed from (1, 2) to (3, 4)) when these images were processed using either the image processing pipeline (D) or image processing pipeline (E).

There was statistically significant difference between the proportions of images with image quality score 3, obtained with image processing pipeline (D) and image processing pipeline (E) with $P = 0.015$. Similarly, there was statistically significant difference between the proportions of images with image quality score 4, obtained with image processing pipeline (D) and image processing pipeline (E) with P value = 0.015.

Quantitative image quality assessment

The summary statistics of the PIQE value [Table 3] and the result of two-tailed dependent samples sign test between the PIQE score of input image and the PIQE score of images obtained using different image processing

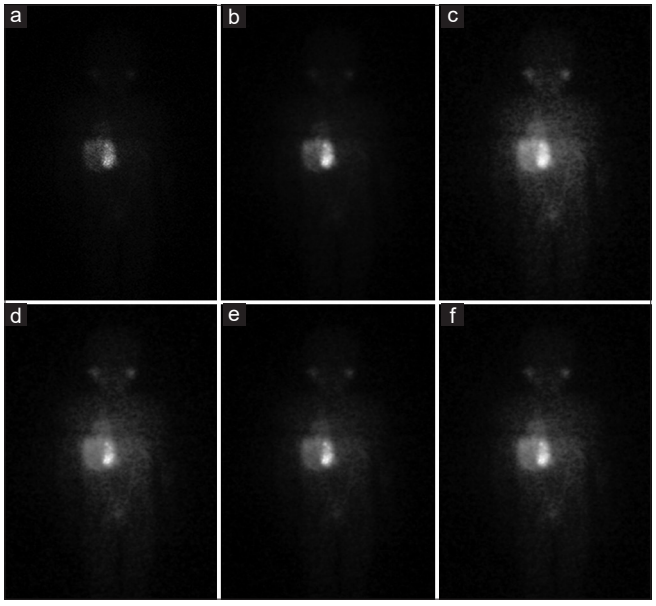

Figure 5: (a) Input image (NMP score = 3, PIQE score = 66.09), (b) output image from image processing pipeline (A) (NMP score = 4, PIQE score = 21.53), (c) output image from image processing pipeline (B) (NMP score = 2, PIQE score = 20.15), (d) output image from image processing pipeline (C) (NMP score = 2, PIQE score = 23.74), (e) output image from image processing pipeline (D) (NMP score = 3, PIQE score = 15.62), (f) output image from image processing pipeline (E) (NMP score = 3, PIQE score = 18.17)

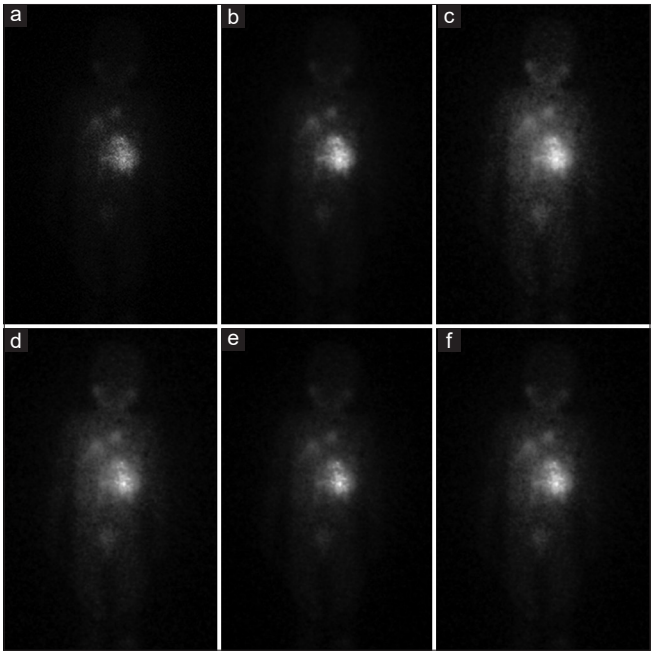

Figure 6: (a) Input image (NMP score = 4, PIQE score = 63.60), (b) output image from image processing pipeline (A) (NMP score: 4, PIQE score = 19.03), (c) output image from image processing pipeline (B) (NMP score = 2, PIQE score = 22.22), (d) output image from image processing pipeline (C) (NMP Score = 2, PIQE score = 23.74), (e) output image from image processing pipeline (D) (NMP score = 3, PIQE score = 15.97), (f) output image from image processing pipeline (E) (NMP score = 3, PIQE score = 20.26)

Table 1: Summary statistics of the image quality score assigned to images obtained using image processing pipelines by nuclear medicine physicians

	Input Image	Image processing pipeline (A)	Image processing pipeline (B)	Image processing pipeline (C)	Image processing pipeline (D)	Image processing pipeline (E)
Mean±SD	1.78±0.79	2.68±0.65	2.72±0.48	2.81±0.42	3.73±0.44	3.58±0.49
Median	2	3	3	3	4	4
Minimum	1	2	2	2	3	3
Maximum	4	4	4	4	4	4

SD: Standard deviation

Table 2: The number of times a particular image quality score assigned to input and output images obtained using different image processing pipelines (A, B, C, D, and E)

Image Quality Score	Input Image	Images obtained using image processing pipeline (A)	Images obtained using image processing pipeline (B)	Images obtained using image processing pipeline (C)	Images obtained using image processing pipeline (D)	Images obtained using image processing pipeline (E)
1	53	-	-	-	-	-
2	43	51	35	24	-	-
3	25	58	85	96	32	51
4	1	13	2	2	90	71

Table 3: Summary statistics based on perception-based image quality evaluator score

	Input image	Image processing pipeline (A)	Image processing pipeline (B)	Image processing pipeline (C)	Image processing pipeline (D)	Image processing pipeline (E)
Mean±SD	79.83±6.03	21.30±3.49	27.44±4.49	26.69±4.54	25.32±5.37	26.32±5.38
Median	81.30	21.31	27.74	26.43	24.55	25.83
Range	52.25-88.83	12.48-29.91	14.99-41.61	12.75-35.65	14.39-44.39	13.80-40.21

SD: Standard deviation

Table 4: Result of two-tailed dependent samples sign test between the perception-based image quality evaluator score data

	S	Median difference	*P*	CI
Between input image and image obtained using image processing pipeline (A)	122	58.23	2.2e-16	57.12-60.52
Between input image and image obtained using image processing pipeline (B)	122	52.60	2.2e-16	51.98-53.67
Between input image and image obtained using image processing pipeline (C)	122	53.51	2.2e-16	52.65-54.53
Between input image and image obtained using image processing pipeline (D)	122	55.26	2.2e-16	53.84-56.60
Between input image and image obtained using image processing pipeline (E)	122	53.65	2.2e-16	52.94-54.82
Between image obtained using image processing pipeline (D) and image obtained using image processing pipeline (E)	18	−4.48	6.78e-16	−5.17-−3.83

The symbol S signifies the S-statistic (the number of positive differences between the data and the hypothesized median. Hypothesized median value was kept equal to 0. S equal to 18 (bottom row, 2nd column) which indicates that 18 (out of 122) images obtained with image processing pipeline D had higher PIQE score than that of images obtained with image processing pipeline E. That is why median difference (bottom row, 3rd column) and CI range of median difference were negative (bottom row, 5th column). CI: Confidence interval, PIQE: Perception-based image quality evaluator

pipelines [Table 4] show that there was statistically significant difference between image quality of the input image and the image quality of the images obtained using image processing pipelines. The qualities of the image obtained using image processing pipelines were better than the quality of the input image.

Based on the PIQE score also, there was statistically significant difference between the image quality score of the image obtained using image processing pipeline (D) and image processing pipeline (E), and the negative value of median difference indicates that in majority of cases, PIQE score of image obtained using image processing pipeline (D) was less than that of images obtained using image processing pipeline (E). The value of the S-statistic (the number of positive differences between the data and the hypothesized median), in this case, was found to be 18; it means that there were 18 images in which the image quality score of the images obtained using image processing pipeline (D) was greater

than that of image obtained using image processing pipeline (E).

The PIQE value of majority of images obtained using image processing pipeline (D) and image processing pipeline (E) is <35, and PIQE value of input images is above 60 [Figure 7] which indicates that perceptual quality of images obtained using image processing pipeline (D) and image processing pipeline (E) was better than its input images. It is to be remembered smaller the value of PIQE better perceptual image quality.[17]

This result is also in consistent with the visual image quality assessment made by the nuclear medicine physicians. However, based on median value of PIQE score, the images obtained using image processing pipeline (A) has best perceptual image quality.

In brief, the image quality obtained with all the five image processing pipelines (A, B, C, D, and E) was better than input images. Based on PIQE score, the performance of image processing pipeline A was maximum and the performance of image processing pipeline B was minimum. Based on PIQE score, the performance of image processing pipeline in decreasing order is image processing pipeline A, D, E, C, and B. Based on visual assessment, the performance of image processing pipeline in decreasing order is: image processing pipeline D, E, A, C, and B.

Discussion

The goal of image enhancement is to improve the image quality so that the processed image is better than the original image for a specific application or set of objectives.[3] The objectives could be to improve the interpretability or perception of information for human eyes or to provide better input for other automated image processing techniques. Histogram transformation is considered as one of the fundamental processes for contrast enhancement of gray level images, which facilitates subsequent higher level operations such as detection and identification.[3,4,5,12] Gaussian filters remove noise from the image and improve signal to noise.[3-5] The minimum and maximum pixel value (i.e., counts) in the output image (obtained with different image processing pipeline) might not be same. Hence, it will be difficult to compare the image quality yielded by different image processing pipeline. Therefore, we applied normalization techniques so that the minimum and maximum counts in the output image (obtained with different image processing pipeline) are 0 and 1, respectively (i.e., same minimum and maximum counts). This makes the comparison of performance of different image processing pipeline reliable.

In this study, we created five different image processing pipelines [A, B, C, D, and E, Figure 2] and evaluated their performance both objectively and subjectively for enhancing the quality of I-131-MIBG images. There was a discordance in the selection of best image processing pipeline based on *PIQE* score (the best image processing pipeline A) and on image quality score assigned by nuclear medicine physician (the best image processing pipeline D). Image processing pipeline D was second only to pipeline A in PIQE score; however, scored higher since other anatomical details available in the image was also considered in the visual scoring by the nuclear medicine physician. Thus, selection made by nuclear medicine physician was considered as the best image processing pipeline. Hence, the performance of image processing pipeline D was found to be better compared to all other image processing pipeline. The quality of the images obtained using image processing pipeline D was also statistically significant than that of the input images ($P < 0.00001$).

The image processing pipeline E performed well but not method A based on visual assessment. Image processing pipeline A does not use histogram specification while image processing pipeline E uses histogram specification technique. Application of histogram specification technique has modified the intensity distribution of the histogram. This has resulted in improved contrast and also information hidden in low count as well as high counts are more clearly visible in image (obtained with method E) compared to

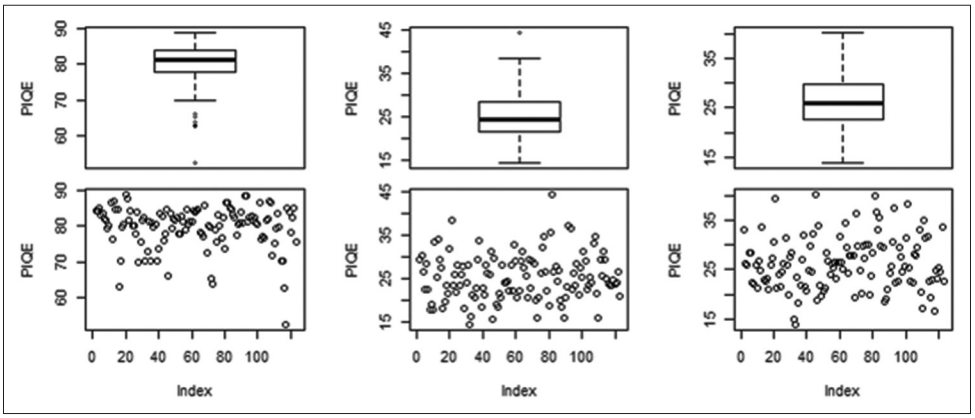

Figure 7: Simple plots and box plot of PIQE score for input image (left column), images obtained using image processing pipeline (D) (center column), and images obtained using image processing pipeline (E) (right column)

image (obtained with method A) [compare the Figures 5b and f and 6b and f]. The improved contrast and more clearly visible information in both dark and bright region in the images obtained with image processing pipeline E might be the reason for preference of image processing pipeline E over image processing pipeline A.

I-131-MIBG image is relatively dark (high concentration of low gray levels in the histogram) and also noisy [because of low pixel counts, for example: maximum pixel counts = 26, Figure 1]. Hence, our ideas were to apply histogram specification to spread the gray levels of histogram so that the quality of output image becomes similar to one of the images displayed in Figure 3, and then, apply Gaussian filters of small radius (i.e., $\sigma = 1$ pixel); the application of the Gaussian filter will ensure an optimally smooth image without loss of significant image details. Since the application of Gaussian filters might also modify the dynamic range of the gray levels, the normalization of the gray levels in the range (0, 1) was performed, so that display monitor faithfully displays all the information available in the image.

The literature available on the quality of I-131-MIBG image or I-131 whole-body image is very limited, and especially, using the image processing pipelines, the combination of histogram specification, Gaussian filter, and normalization of gray levels is not available. Therefore, we could not discuss the comparison of our study with other published literature. However, we are including the brief review of the literatures available on the improvement of quality of I-131 image.

Pandey *et al*.[19] performed denoising of I-131 images using median filter; in this study, they have compared the performance of a plus-shape and a square-shape median filter for I-131 whole-body images. The plus-shape median filter was found to show better performance in comparison with the square-shape median filter. The plus-shape median filter with a mask size of 7 pixels was found to be optimum for the processing of whole-body I-131 images. Pandey *et al*.[20] also performed another study for the improvement of I-131 whole-body scan. The aim of the study was to restore I-131 whole-body image using Wiener filter. The restored images with plus-shape median filter (size = 13, sigma = 2) and noise-to-signal power ratio = 0.3 were found to have superior image quality in comparison with its input image.

This pipeline can be utilized to enhance the quality of I-131-mIBG image if the images have been acquired following the same acquisition protocol used in this study. The change in acquisition protocol might require another image processing pipeline.

The principle of using a pipeline of image processing techniques to solve a complex image enhancement task is not new; however, the idea of selecting a list of image processing tasks (histogram specifications, Gaussian blur, and normalization) and then combining them into a sequence so that problem of I-131-mIBG image enhancement can be solved is our original idea.

Image denoising is a well-developed topic in low-level vision. Many approaches have been proposed, using techniques such as total variation,[21] wavelet-domain processing,[22] sparse coding,[23,24] nuclear norm minimization,[25] and 3D transform-domain filtering (BM3D).[26] The 3D transform-domain filtering algorithms have been found to be superior compared to recent techniques on real images.[27] Similarly, for low-light image enhancement, a variety of techniques (other than histogram modification which balances the histogram of the entire image) has been developed to enhance the contrast of low-light images (gamma correction, which increases the brightness of dark regions while compressing bright pixels, inverse dark channel prior,[28,29] the wavelet transform,[30] the Retinex model,[31] and illumination map estimation[32]) that can be used for I-131-mIBG images.

The limitation of the study is that it has only considered histogram specification, Gaussian filtering, and normalization techniques to include in the pipeline, the list of a large amount of literature is available on image processing techniques.[21-32] Further, theoretically, there exist many possible permutations and combinations with these three image processing techniques, for example, histogram specification requires input as the histogram (unlimited number of histogram can be assigned), similarly the performance Gaussian filter depends on the radius (standard deviation) and the size of the window, and in this case, also many possible combination of input parameters exists).

Our image processing pipeline did not involve the state-of-art algorithm for image denoising and also the advanced technique developed for low-light image enhancement. The presented work opens many opportunities for future research. A better image processing pipeline can be developed in future using these latest image processing techniques.

Designing and optimizing new image processing pipeline is time-consuming and costly.[33] The researchers have focused their attention on automation of designing and optimizing image processing pipeline.[11,33-35]

We would like to further improve the image quality of I-131-mIBG image by designing and optimizing new image processing pipeline using state-of-art algorithm for image denoising and also using the advanced image processing techniques developed for low-light image enhancement. During this process, we would like to adopt the procedure for automating the designing and optimizing image processing pipeline developed in the literature,[11,33-35] to reduce the time and cost involved in designing and optimizing image processing pipeline.

Conclusions

The image quality of I-131-MIBG scan was improved significantly using the image processing pipeline D involving the following image processing techniques in sequence: histogram specifications, Gaussian blur of 1 pixel radius, and normalization.

Financial support and sponsorship

Nil.

Conflicts of interest

There are no conflicts of interest.

References

1. Agrawal A, Rangarajan V, Shah S, Puranik A, Purandare N. MIBG (metaiodobenzylguanidine) theranostics in pediatric and adult malignancies. Br J Radiol 2018;91(1091):20180103. doi: 10.1259/bjr.20180103. Epub 2018 Aug 13.
2. Franzius C, Hermann K, Weckesser M, Kopka K, Juergens KU, Vormoor J, *et al*. Whole-body PET/CT with 11C-meta-hydroxyephedrine in tumors of the sympathetic nervous system: Feasibility study and comparison with 123I-MIBG SPECT/CT. J Nucl Med 2006;47:1635-42.
3. Gonzales RC, Woods RE. Digital Image Processing. New Jersey: Prentice Hall; 2002.
4. Bovik AC. Handbook of Image and Video Processing. San Diego, London: Academic Press; 2000.
5. Jähne B. Digital Image Processing. Berlin, New York: Springer Verlag; 2002.
6. Mencattini M, Salmeri R, Frigerio LM, Caselli F. Mammographic images enhancement and denoising for breast cancer detection using dyadic wavelet processing. IEEE Trans Instrum Meas 2008;57:1422-30.
7. Scharcanski J, Jung CR. Denoising and enhancing digital mammographic images for visual screening. Comput Med Imaging Graph 2006;30:243-54.
8. Tsai DY, Lee Y, Chiba R. "An Improved Adaptive Neighbourhood Contrast Enhancement Method for Medical Images," In Proceedings of the 3rd IASTED International Conference on Medical Engineering, BioMed; February 2005. p. 59-63.
9. Yoon BW, Song WJ. Image contrast enhancement based on the generalized histogram. Journal of electronic imaging. 2007 Jul;16(3):033005.
10. Fodor IK, Kamath C. Denoising through wavelet shrinkage: An empirical study. J Electron Imaging 2003;12:151-60.
11. Chen C, Chen Q, Xu J, Koltun V. Learning to See in the Dark. In Proceedings of the IEEE Conference on Computer Vision and Pattern Recognition; 2018. p. 3291-300.
12. Pandey AK, Sharma PD, Sharma A, Negi A, Parida GK, Goyal H, *et al*. Improving technetium99m methylene diphosphonate bone scan images using histogram specification technique. World J Nucl Med 2020;19:224-32.
13. R Core Team. R: A Language and Environment for Statistical Computing. Foundation for Statistical Computing, Vienna, Austria; 2018. Available from: https://www.R project.org/. [Last accessed on 2020 Dec 01].
14. Barthelme S. Imager: Image Processing Library Based on 'CImg'. Package Version 0.42.3; 2020. Available from: https:// CRAN.R project.org/package=imager. [Last accessed on 2020 Dec 01].
15. Pau G, Fuchs F, Sklyar O, Boutros M, Huber W. EBImage – An R package for image processing with applications to cellular phenotypes. Bioinformatics 2010;26:979-81.
16. Venkatanath N, Praneeth D, Chandrasekhar BH, Channappayya SS, Medasani SS. Blind Image Quality Evaluation Using Perception Based Features. In Proceedings of the 21st National Conference on Communications (NCC). Piscataway, NJ: IEEE; 978-1-4799-6619-6/15; 2015.
17. Matlab. Available from: https://in.mathworks.com/help/images/ref/piqe.html. [Last accessed on 2019 Jan 10].
18. Arnholt AT, Evans B. BSDA: Basic Statistics and Data Analysis. Package Version 1.2.0; 2017. Available from: https:// CRAN.R-project.org/package=BSDA. [Last accessed on 2021 Feb 09].
19. Pandey AK, Sharma A, Sharma PD, Saroha K, Parida GK, Bal CS, *et al*. Denoising of iodine-131 images using a median filter. Nucl Med Commun 2019;40:308-16.
20. Pandey AK, Santosh Y, Sharma PD, Yadav D, Bal C, Kumar R. Restoration of I-131 whole body image using a Wiener filter. Nucl Med Commun 2020;41:426-35.
21. Rudin LI, Osher S, Fatemi E. Nonlinear total variation based noise removal algorithms. Physica D: nonlinear phenomena. 1992 Nov 1;60(1-4):259-68.
22. Portilla J, Strela V, Wainwright MJ, Simoncelli EP. Image denoising using scale mixtures of gaussians in the wavelet domain. IEEE Tran Image Process 2003;12:1338-51.
23. Elad M, Aharon M. Image denoising via sparse and redundant representations over learned dictionaries. IEEE Trans Image Process 2006;15:3736-45.
24. Mairal J, Bach F, Ponce J, Sapiro G, Zisserman A. "Non-Local Sparse Models for Image Restoration," 2009 IEEE 12th International Conference on Computer Vision, Kyoto; 2009. p. 2272-9.
25. Gu S, Zhang L, Zuo W, Feng X. "Weighted Nuclear Norm Minimization with Application to Image Denoising," 2014 IEEE Conference on Computer Vision and Pattern Recognition, Columbus, OH; 2014. p. 2862-9.
26. Dabov K, Foi A, Katkovnik V, Egiazarian K. Image denoising by sparse 3-D transform-domain collaborative filtering. IEEE Trans Image Process 2007;16:2080-95.
27. Plötz T, Roth S. Benchmarking Denoising Algorithms with Real Photographs. 2017 IEEE Conference on Computer Vision and Pattern Recognition (CVPR), Honolulu, HI; 2017. p. 2750-9.
28. Dong X, Wang G, Pang Yi, Li W, Wen J, Meng W, *et al*. "Fast Efficient Algorithm for Enhancement of Low Lighting Video," 2011 IEEE International Conference on Multimedia and Expo, Barcelona; 2011. p. 1-6.
29. Malm H, Oskarsson M, Warrant E, Clarberg P, Hasselgren J, Lejdfors C. "Adaptive Enhancement and Noise Reduction in Very Low Light-Level Video," 2007 IEEE 11th International Conference on Computer Vision, Rio de Janeiro; 2007. p. 1-8.
30. Łoza A, Bull DR, Hill PR, Achim AM. Automatic contrast enhancement of low-light images based on local statistics of wavelet coefficients. Digit Signal Process 2004;23:1856-66.
31. Park S, Yu S, Moon B, Ko S, Paik J. Low-light image enhancement using variational optimization-based Retinex model. IEEE Trans Consum Electron 2017;63:178-84.
32. Guo X, Li Y, Ling H. LIME: Low-light image enhancement via illumination map estimation. IEEE Trans Image Process 2017;26:982-93.
33. Jiang H, Tian Q, Farrell J, Wandell BA. Learning the image processing pipeline. IEEE Trans Image Process 2017;26:5032-42.
34. Lansel, Steven P, Brian A. Wandell. Learning of image processing pipeline for digital imaging devices U.S. Patent No. 8,675,105. 18 Mar. 2014.
35. Schwartz E, Giryes R, Bronstein AM. DeepISP: Toward learning an end-to-end image processing pipeline. IEEE Trans Image Process 2018;28:912-23.